Article

Not peer-reviewed version

Microstructure Evaluation of Cryogenically Hardened and Tempered AISI H13 Hot Work Tool Steel

Dimitrios George Papageorgiou *, Anastasia Alexandratou, Dionysios E. Mouzakis, Costas Charitidis, Dimitrios Manolakos

Posted Date: 25 May 2026

doi: 10.20944/preprints202605.1642.v1

Keywords: hot work tool steel; cryogenic treatment; microstructure evaluation; martensite; primary carbides; nanocarbides; secondary carbides precipitation

 doi:10.20944/preprints202605.1642.v1

Article

Microstructure Evaluation of Cryogenically Hardened and Tempered AISI H13 Hot Work Tool Steel

Dimitrios George Papageorgiou [1,*], Anastasia Alexandratou [2], Dionysios E. Mouzakis [3], Costas Charitidis [2] and Dimitrios Manolakos [1]

[1] School of Mechanical Engineering, National Technical University of Athens, 15780 Zografos, Greece

[2] School of Chemical Engineering, National Technical University of Athens, 15773 Zografos Greece

[3] Department of Military Sciences, Hellenic Army Academy,16673, Vari, Greece

* Correspondence: dimpapg47@mail.ntua.gr

Abstract

The aim of the present study is to demonstrate the microstructure features of AISI H13 hot work tool steel grade after been shallow (SCT) and deep (DCT) cryogenic hardened. Cryogenic hardening is a method of enchancing primarily wear resistance, as well as toughness and corrosion resistance of tool steels. The specific steel grade studied is of high importance as it is the most used in hot work applications as well as to engineering components requiring moderate to high toughness. Initially, groups of SCT and DCT hardened specimens were reheated covering the tempering range of 180^{0}C to 550^{0}C. Metallographic samples after low tempering to 180^{0}C, as well as to the range of tempering temperatures in the vicinity of the secondary hardening peak, namely, 500^{0}C, 525^{0}C and 550^{0}C were investigated by light and scanning electron microscopy. Primary carbides of Cr, V and Mo were found while micron and nanocarbides were found in both SCT and DCT samples. The precipitated carbides are formed on the grain boundaries as well as in-between martensitic laths. Increasing tempering temperature, carbides precipitation is more dispersed along the microstructure and intense to grain boundaries. Lath martensite was observed in both cryogenic procedures.

Keywords: hot work tool steel; cryogenic treatment; microstructure evaluation; martensite; primary carbides; nanocarbides; secondary carbides precipitation

1. Introduction

Subzero treatment is a ecofriendly heat treating process [1,2] which is implemented in a rage of temperatures approximately from -72^{0}C (use of dry ice), -185^{0}C (use of liquid nitrogen) and ultimately to -268^{0}C (use liquid helium) [3]. These treatments can be applied and positively affect materials made of different chemical bonding corresponding to metals (steels, Al, Cu, Mg alloys), carbides, polymers and metallic glasses [4,5]. Based on these temperatures, in case of steels, it can be grossly categorized as a) cold treatment when the treating temperature reaching a down limit of -80^{0}C, b) shallow cryogenic treatment which is labeled when the treatment temperatures are in the range of -80^{0}C to -160^{0}C and c) the deep cryogenic treatment extending down to -196^{0}C [6–12]. The process is based on microstructure alterations due to applied subzero temperatures resulted to substantially increase of the population and distribution of transition carbides forming at low tempering temperatures [13].

The metallurgical transformation occurred during cryotreatment stage is strongly dependent on the subzero temperature selected as well as on the holding time at that temperature. A hybrid model seems to adequately describe the precipitation mechanism of the transition carbides during low temperature tempering. The debated findings of carbon clustering before ε-carbide exerted by one dimensional atom probe tomography by Taylor et al [14] were verified by using three dimensional atom probe by Zhu et al. [15]. On the other hand, the classical model of the heterogeneous nucleation

 doi:10.20944/preprints202605.1642.v1

of ε-carbides is also supported by different researchers [16–18]. Analyzing and synthesizing researchers' findings, carbon clustering (spinodal-like or segregation controlled) produces precursors which are followed by nucleation and growth of ε-carbides. The aforementioned mechanism takes advantage of subzero treatment, so the density and distribution of transition carbides is enhanced. Increased ε,η-carbides precipitation along with the austenite-to-martensite transformation in subzero temperatures is likely to be the main causes of the improved properties of alloyed steels after cryogenic treatment.

In case of tool steel grades, their response to the cryogenic treatment is varying as it depends on their chemical composition especially in carbon and alloying elements additions (Cr, Mo, V, W, Co) as well as on their heat treatment history [19]. According to weight percentage of carbon and of alloying elements, strength [6,20], toughness [21,22], wear [23] and corrosion resistance [24,25] are enhanced [26] respectively. A plot of temperature as function of time for a typical deep cryogenic treatment cycle is demonstrated in Figure 1 [3]. Subzero treatment is an additional process which can be applied in different stages of the heat treatment sequence, namely, between quenching and tempering, between tempering stages or after tempering. Moreover, it can be implemented in more than one cycle, sequential or not [26]. Evidently, in order cryogenic treatments to be effective they need to be carried out after martensitic quenching and before tempering [1,27–29].

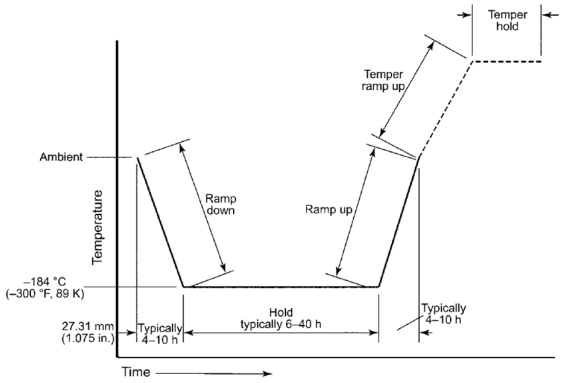

Figure 1. Typical sequence of a deep cryogenic treatment.

In a more practical manner, the working life improvement of engineering components constructed of tool steel grades is given hereunder:

Table 1. Examples of tool life improvement using cryotreatment [30–33].

Tooling	Initial Average working life	Average working life after cryotreatment
5-cm end mils used to cut C1065 steel	65 parts	200 parts
Hacksaw blades used to cut bosses on M107 shells	4h	6h
Zone punches used on shell casings	64 shells	5820 shells
Nosing thread dies used in metal working	225 shells	487 shells
Copper resistance welding tips	2 weeks	6 weeks
Progressive dies used in metal working	40.000 hits	250.000 hits
Blanking of heat treated AISI 4140 and 1095 steel	1.000 pieces	2.000 pieces
Broach used on a C1020 steel torque tube	1.810 parts	8.602 parts
Broaching operation on forged connecting rods	1.500 parts	8.600 parts
Gang milling T-nuts constructed from C1018 steel	3 bars	14 bars
with M2 cutters AMT-38 cut-off blades	60h	928h

 doi:10.20944/preprints202605.1642.v1

In all the above cases of tooling, a heat treatment sequence was implemented, comprising of quenching, subzero treatment and tempering stages. The early research, especially after 2005 and actual industry usage have proven the validity of the cryogenic process, research now is turning to determine why the results are seen and how to maximize those results [34]. Until now, there are many ambiguities in parameters like austenitizing temperature, quenching temperature, rate of cooling, temperature and holding period of subzero treatment, rate of warming-up, tempering temperatures and tempering period. There is need of further investigations so to optimize the parameters of deep cryogenic treatment process for different materials [35]. The improvement in mechanical properties by cryogenic processing is directly related to the combined effect of hardened and tempered martensitic matrix and carbides which are distributed in the microstructure. The austenite-to-martensite transformation, the starting temperature of carbide nucleation during warming up and the tempering sequence regulates the final microstructure of the material. In tool steel grades, the mix of carbides present in the tempered martensite matrix after the cryogenic treatment sequence are critical for their hardness, toughness and the wear resistance respectively [35–37]. The formation mechanism of carbides depend on the tempering behavior of each steel grade and the specific effect must be taken into account when designing their heat treatment sequence tailoring the properties of products [38].

Differences in tempering behavior after cryogenic heat treatment sequence of medium to high alloyed tool steel grades e.g. the temperature of secondary hardening peak has been reported [6,39–42]. The tempering diagrams of tool steel grades should be updated including their behavior after cryogenic treatment so the benefits of the specific treatment to be obtained constantly [43,44].

The tempering diagram of AISI H13 tool steel in the range of 180^{0}C to 630^{0}C has been constructed for different holding times and ramp up rates in shallow and deep cryogenic temperatures [45]. A comparative tempering diagram of H13 tool steel grade is demonstrated in Figure 2. During tempering of tool steels, there can be six overlapping stages of carbides evolution as temperature increases [41,46,47]:

Stage 0: carbon clustering starting from subzero temperatures to 150^{0}C,

Stage 1: precipitation of transition carbides, extended between 150^{0}C to 230^{0}C,

Stage 2: austenite decomposition, mainly occurring between 230^{0}C to 280^{0}C presenting critical overlapping on both previous and followed stage,

Stage 3: in situ transformation of transition carbides to cementite, 260^{0}C to 360^{0}C,

Stage 4: heterogenous nucleation of alloy carbides provoking secondary hardening, 450^{0}C-550^{0}C,

Stage 5: coarsening of precipitated carbides, 550^{0}C-650^{0}C.

Tempering the tool steel over 350^{0}C approximately is accompanied by a gradual decrease in hardness and tensile strength due to the loss of tetragonality of martensite and the escape of carbon from solid solution to form cementite. At higher tempering temperatures, a further decrease of hardness is caused by the coarsening of cementite and recrystallization of ferrite.

According to various researchers [48–53] in case of hardening H13 tool steel, primary carbides M_7C_3, M_6C and MC are expected to be present after austenitizing and quenching. Cryotreating and low tempering lead to in-situ nucleation of M_3C carbides on ε/η transition carbides. During secondary hardening, M_3C carbides transform to Cr rich M_7C_3 and Mo rich M_2C carbides respectively. Moreover, prolonged or repeated tempering lead M_7C_3 and M_2C carbides to transform to more stable carbides $M_{23}C_6$ and M_6C respectively.

 doi:10.20944/preprints202605.1642.v1

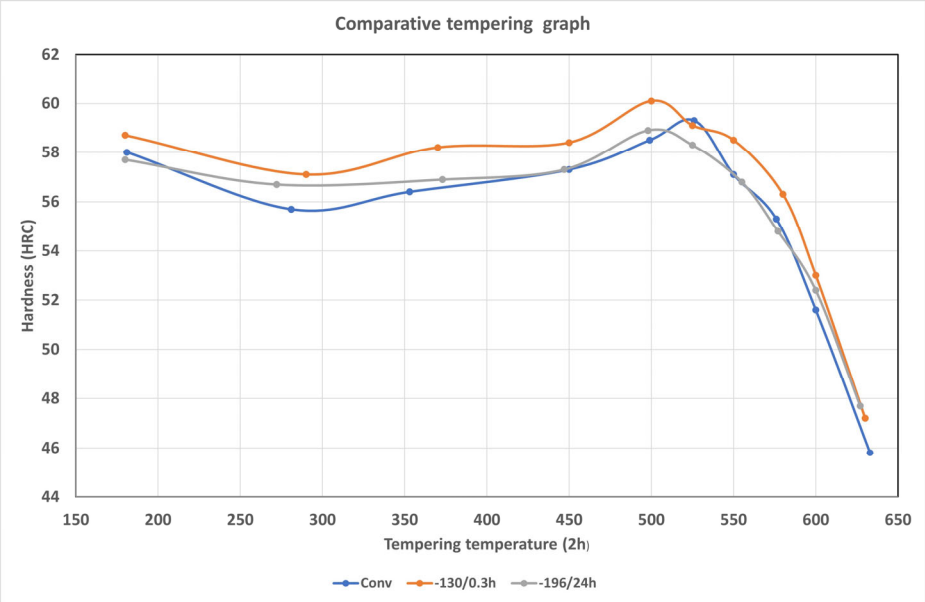

Figure 2. Tempering diagram of H13 tool steel after conventional, shallow and deep cryogenic treatment.

In all the cases above, the austenitizing temperature was set to 1040^{0}C and the soaking time was 30 min. All specimens were air cooled, and snap tempered to 100^{0}C for 1 hour. Then the actual tempering time was 2h. In shallow cryogenic treatment, the temperature was held to -130^{0}C for 30 min and the warming up duration was 30h (inside the cryogenic chamber). Moreover, in case of deep cryogenic treatment, the temperature was hold to -196^{0}C for 24h and the warming up duration was 1h respectively. Differences between the conventional and cryogenic tempering diagrams have been reported e.g. the secondary hardness peak appeared in lower tempering temperature [39,40] or the secondary hardening been suppressed due to DCT [13,20]. Evidently, holding time to subzero temperature affects the tempering behavior of the tool steel in the range of secondary hardness [54].

The microstructural features of cryogenically treated and tempered H13 tool steel have been extensively demonstrated by various researchers using different heat treatment parameters as a) the austenitizing and tempering temperatures, b) the temperature and holding time of the subzero treatment, c) the position of the subzero treatment related to quenching and tempering based on the aim of their study [48–50,55–58]. Consequently, the documentation of the microstructure demonstrated by different researchers has been extracted for different heat treatment parameters without following specific patterns. The scope of the specific labor is to examine the evolution of the microstructure features acquired after shallow and deep cryogenic treatment under the same conditions so the results to be reproducible. Material of the same melt as well as heat treatment equipment e.g. for austenitizing, quenching, subzero treatment and tempering were used. Different tempering temperatures were chosen so the evolution of the microstructure to be demonstrated. Its features were documented via optical and scanning electron microscopy. A comparison of the microstructure of cryogenically shallow and deep cryogenic treated specimens covering critical tempering temperatures in the range of 180^{0}C to 630^{0}C is discussed.

2. Materials and Methods

2.1. Material and Treatment

A chromium-molybdenum-vanadium-alloyed having medium carbon %wt steel grade was used belonging to hot work tool steels family. AISI H13 has an exceptional combination of mechanical properties,namely, high level of toughness and ductility, uniform and high level of machinability and polishability, good resistance to abrasion at both low and high temperatures, good high-temperature strength and resistance to thermal fatigue, excellent through-hardening properties and very limited

 doi:10.20944/preprints202605.1642.v1

distortion during hardening [59]. The cast analysis of the plate used for the construction of the specimens is given in Table 2.

Table 2. Cast analysis of the tool steel samples used in wt%.

Chemical composition (% wt.)	C	Si	P	S	Cr	Mo	V
Cast analysis	0,39	1,01	0,017	0.0006	5,15	1,28	0.91

Forty specimens of dimensions 15x15x40mm divided in two equal batches, A (shallow cryogenic treatment) and B (deep cryogenic treatment). In sequential time periods were heated in a muffle furnace at a rate of 25◦C/min approximately to austenitizing temperature of 1040◦C. The soaking time for both treatments was the same, equal to 30 min. The specimens were wrapped with distilled paper and placed in a steel box so to prevent decarburization in case of direct contact with the atmosphere of the furnace. In both cases, the specimens were quenched via pressurized air. Immediately after quenching, all samples were snap tempered to 100◦C for 1h [60]. The specimens of batch A were cryotreated to -130◦C, holding time of 20min, having ramp up duration of 30h (physically warmed to ambient temperature inside the cryogenic chamber) as the specimens of batch B were cryotreated to -196◦C for 24h respectively using liquid nitrogen via cryogenic chamber (Cryotron LTI 40). The cooling rate was relatively slow to 2,5◦C/min.

A couple of specimens was used in each one of the ten temperatures selected so the evolution of microstructure and hardness during the range of 180◦C to 630◦C to be studied. The temperatures used for the specific study were 180^{0}C, 280^{0}C, 350^{0}C, 450^{0}C, 500^{0}C, 525^{0}C, 550^{0}C, 575^{0}C, 600^{0}C, 630^{0}C respectively covering all sequential stages of tool steels tempering. The duration of each tempering stage was 2h. In the present study, the evolution of the microstructure after low tempering to 180^{0}C, as well as to the vicinity of secondary hardening temperature of the specific tool steel grade,namely, 500^{0}C, 525^{0}C and 550^{0}C is implemented.

2.2. Method

One of the two specimens of each heat treatment sequence (austenitized, quenched cryotreated, snap tempered and tempered) was prepared for microhardness testing [61] and the other for metallographic analysis respectively [62]. Four specimens of each of the two subzero treatmets which were tempered at 180^{0}C, 500^{0}C, 525^{0}C, 550^{0}C, were cut, cold mounted and grinded using sequal grinding papers starting form P#80 to P#2000 grit size. Then, they were polished with alumina paste and emulsion of 6, 3, 1 and 0,3μm grain size sequentially. The microstructure analysis was held after etching the specimens with 5% Nital. Optical microscope Zeiss Axio Vert A1 as well as scanning electron microscopes (Jeol JSM-6390, Jeol JSM-7610F, Hitachi TM3030Plus) were utilized to depict the microstructural evolution of the cryotreated material.

3. Results and Discussion

3.1. Low Tempering

Optical microscopy of specimens subjected to deep (-196^{0}C, hold for 24h, ramp up duration 1h, Figure 3a,b) and shallow (-130^{0}C, hold for 0,3h, ramp up duration 30h, Figure 3c,d) cryotreatement, and low tempering to 180^{0}C was employed. The microstructure of both subzero treatments is comprised of matrix of tempered lath martensite (Figure 3a, area I, Figure 3c, area III) [63] having acicular areas due to low tempering temperature, of dispersed carbides (Figure 3b, Figure 3d area III)) as well as of retained austenite (Figure 3b area II) [64].

 doi:10.20944/preprints202605.1642.v1

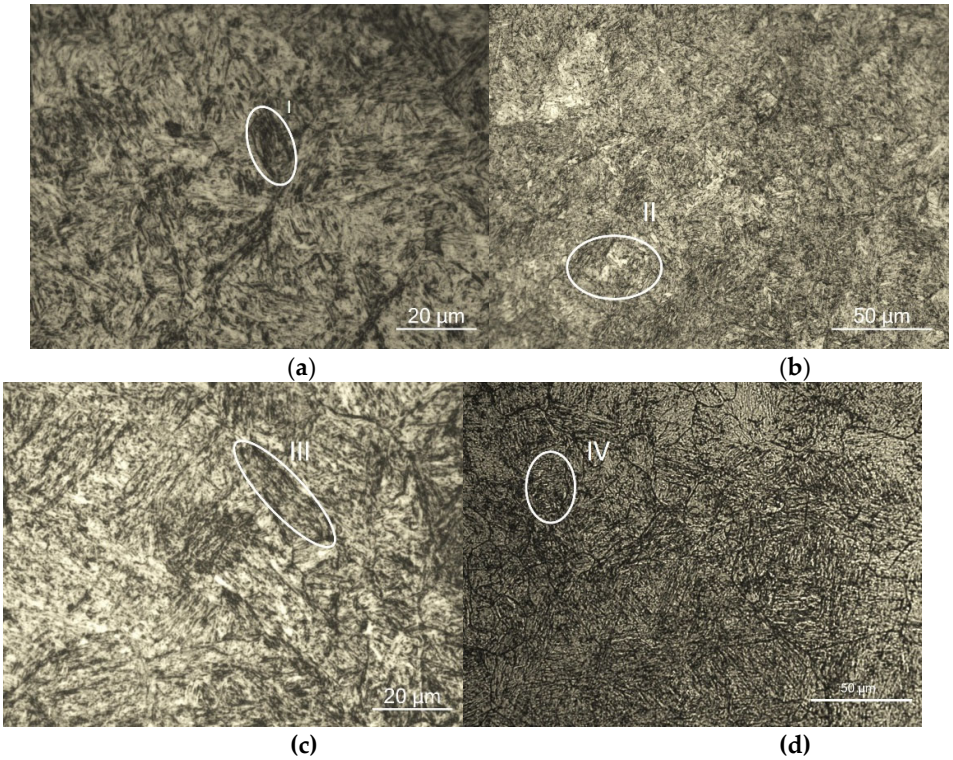

(**a**) (**b**)

(**c**) (**d**)

Figure 3. Microstructure of medium carbon Cr-Mo-V alloyed tool steel after hardening, cryotreating and low tempering: (**a**) Laths of tempered martensite; (**b**) Dispersed carbides and retained austenite in a matrix of tempered martensite, (**c**) Tempered martensite laths; (**d**) Dispersed carbides in a matrix of tempered martensite.

In case of the deep cryotreated treatment a more detailed depiction of the features of lath martensite was elaborated using scanning electron microscope verifying the results from optical microscopy (Figure 4).Very fine dispersed sub-micron carbides in the matrix of tempered martensite are depicted [49]. Based on their size and the heat treatment sequence implemented transition (Figure 4a, area I)[65] and primary carbides are present (Figure 4a, area II) [24,26,66]. An element mapping via energy-dispersive X-ray spectroscopy was elaborated on the same specimen. Primary V, Cr and Mo rich carbides of were detected (Figure 4b).

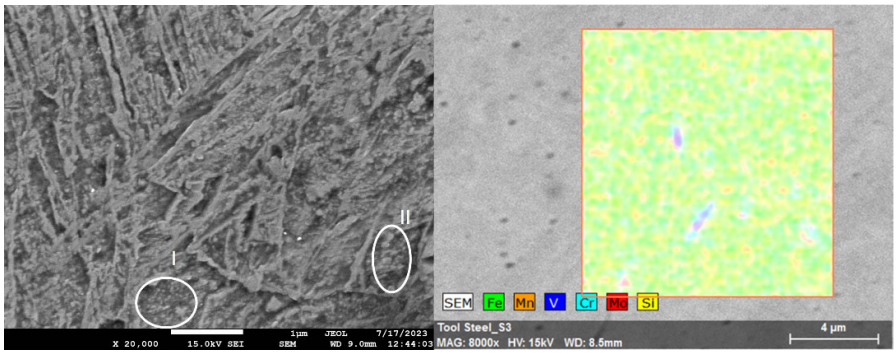

(**a**) (**b**)

Figure 4. Microstructure of medium carbon Cr-Mo-V alloyed tool steel after hardening, deep cryotreating and low tempering: (**a**) Laths of tempered martensite; (**b**) Dispersed primary carbides in a matrix of tempered martensite.

Moreover, detailed observation on both microstructures via scanning electron microscope revealed carbide colonies located to the grain boundaries and globular sub-micron carbides

 doi:10.20944/preprints202605.1642.v1

precipitated inside the grains after shallow (Figure 5a) and deep cryogenic treatment respectively (Figure 5b) [26].

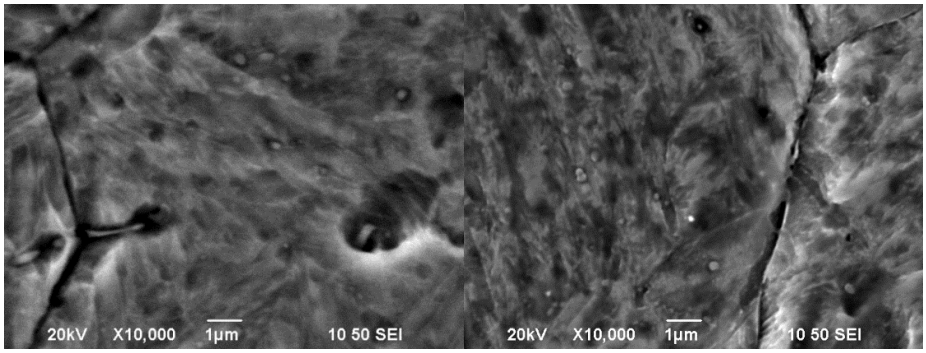

(**a**) (**b**)

Figure 5. Carbides formation on the grain boundaries and their distribution inside the grains: (a) deep cryotreated-low tempering treatment; (b) shallow cryotreated-low tempering treatment.

3.2. Tempering at 500^{0}C

On both tempering diagrams constructed for shallow (-130^{0}C/0,3h) and cryogenic (-196^{0}C/24h) treatment of the specific tool steel grade (Figure 2) it presents secondary hardening peak.

The microstructure extracted by optical microscope of both deep (Figure 6a,b) and shallow (Figure 6c,d) cryotreated and tempered at 500^{0}C samples, it is comprized of tempered martensite (Figure 6a,c) and dispersed carbides (Figure 6b,d). There is no clear evidence of the presence of retained austenite so its weight percent is expected to be less than 5%.

In case of deep cryogenic treatment, the matrix of tempered martensite has more distinct grain boundaries related to its morphology after shallow cryogenic treatment. Moreover, carbide precipitation is more pronounced on the grain boundaries after deep cryogenic treatment while in case of shallow cryogenic treatment, carbides are homogenically dispersed inside the matrix of the tempered martensite.

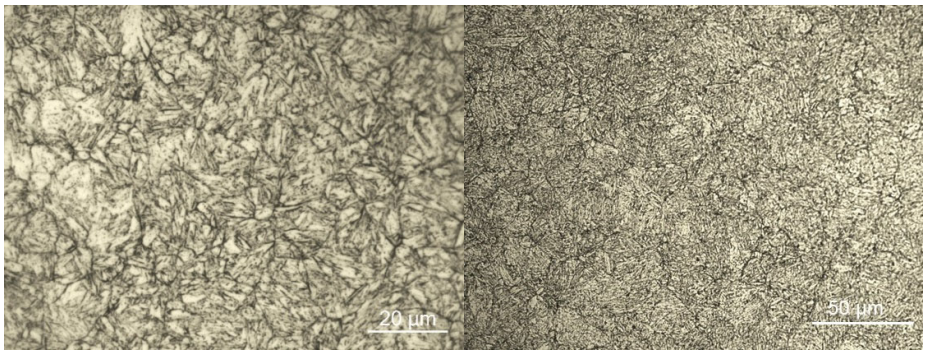

(**a**) (**b**)

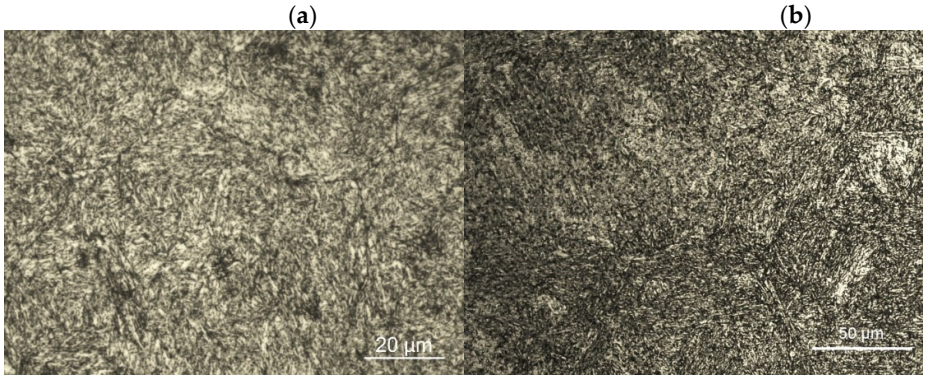

(c) **(d)**

 doi:10.20944/preprints202605.1642.v1

Figure 6. Microstructure revealed via optical microscope after hardening, cryotreating and tempering at 500^{0}C: (**a**) DCT- Distinct grain boundaries of tempered martensite; (**b**) DCT- Precipitated carbides mainly on the grain boundaries of tempered martensite, (**c**) SCT- Tempered martensite matrix; (**d**) SCT- Homogenically dispersed carbides in a matrix of tempered martensite.

In case of deep cryogenic treatment and tempering at 500^{0}C, the grain boundaries of tempered martensite were examined further. Extensive precipitation of secondary carbides was observed (Figure 7).

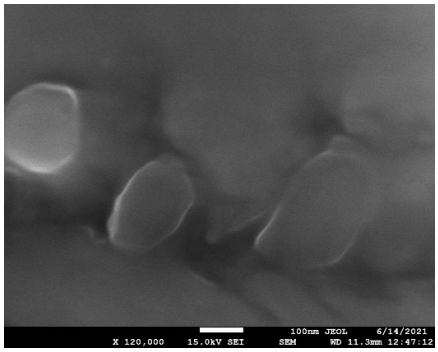

Figure 7. Deep cryogenically treated and tempered at 500^{0}C specimen: carbides precipitation on the grain boundaries of tempeted martensite.

Using scanning electron microscope, sub-micron carbides are precipitated between the laths of tempered martensite in both subzero treatments (Figure 8) [67]. Through the elaborated microstructures, it is evident that the precipitation of interlath carbides is more intense in case of shallow cryotreatment and tempering at secondary hardening peak temperature related to deep cryotreatment respectively. The specific findings are verified by other researchers [56].

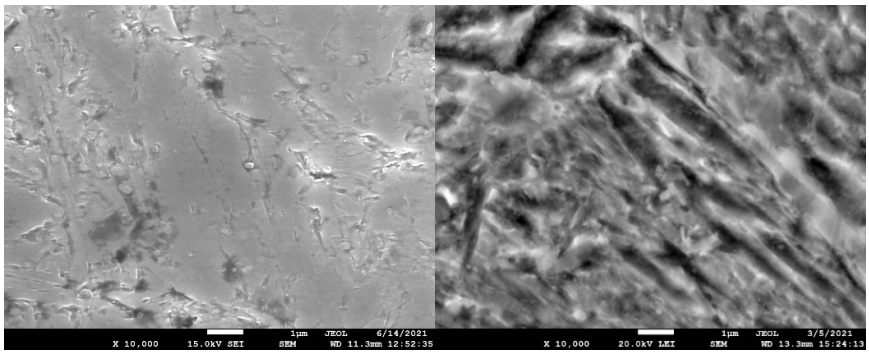

(**a**) (**b**)

Figure 8. Interlath carbides after subzero treatment and tempering to 500^{0}C: (**a**) deep cryogenic hardened and tempered; (**b**) shallow cryogenic hardened and tempered.

3.3. Tempering at 525^{0}C

Through light optical microscopy, the main feature that can observed to the microstructure after tempering at 525^{0}C is the formation of cementite within the tempered martensite phase [68,69] which, by comparison, is more homogenous after deep cryogenic treatment (Figure 9b,d).

 doi:10.20944/preprints202605.1642.v1

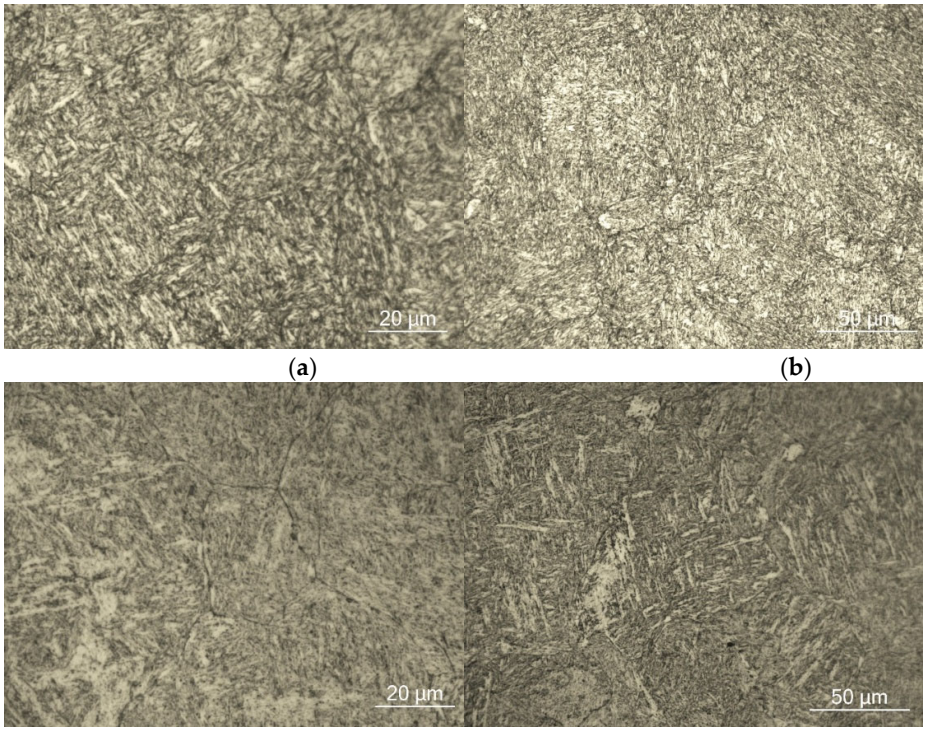

(**a**) (**b**)

(**c**) (**d**)

Figure 9. Acquired microstructure after subzero treatment and tempering at 525^{0}C: (**a,b**) deep cryogenic treatment-homogenous formation of cementite within tempered martensite phase; (**c,d**) shallow cryogenic treatment- inhomogenous formation of cementite within the matrix of tempered martensite.

Carbide precipitation between martensitic laths is noted via scanning electron microscope in both subzero treatments which were tempered at 525^{0}C (Figure 10,11a). Moreover, distinct carbides precipitation is evident on the grain boundaries of shallow cryogenically treated not etched specimen (Figure 11b).

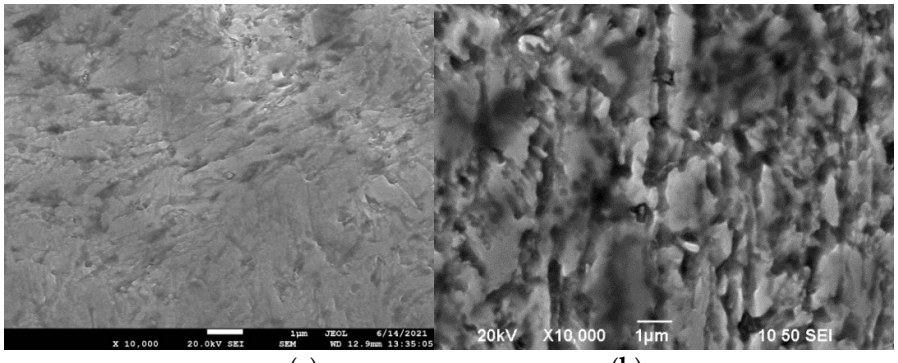

(**a**) (**b**)

Figure 10. Carbide precipitation on martensite laths of quenched, subzero treated and tempered at 525^{0}C hot work tool steel grade: (**a**) deep cryogenic; (**b**) shallow cryogenic treatment.

 doi:10.20944/preprints202605.1642.v1

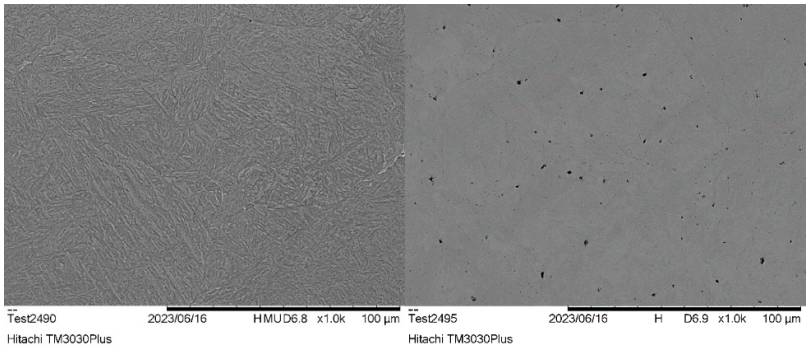

(**a**) (**b**)

Figure 11. Microstructure features of shallow cryogenic treated and tempered at 525^{0}C: (**a**) matrix of tempered martensite with carbide precipitation inside as well as to the boundaries of the grains; (**b**) unetched specimen- carbide precipitates at grain boundaries.

3.4. Tempering at 550^{0}C

Extensive cementite formation as well as coarsening of the precipitated carbides are the main features of the microstructure on both cryotreatments after tempering at 550^{0}C via optical microscopy (Figure 12). In case of shallow cryogenic treatment, the formation of cementite presents inhomogenous areas inside the microstructure and the coarsening of carbides is more evident on the grain boundaries (Figure 12c,d).

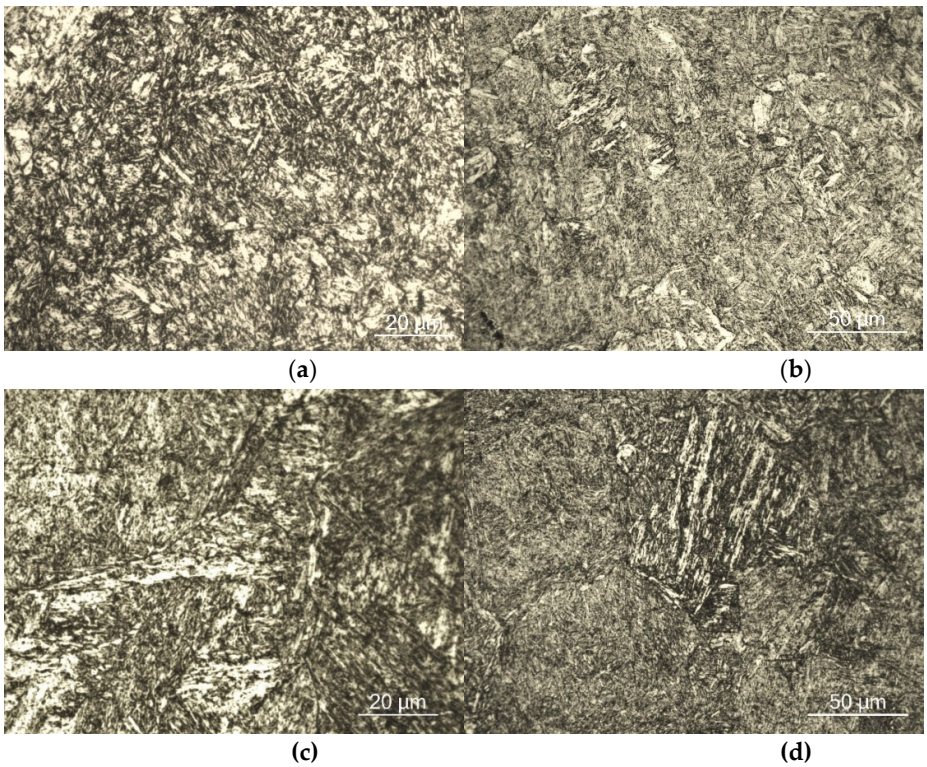

(**a**) (**b**)

(**c**) (**d**)

Figure 12. Microstructure after subzero treatment and tempering at 550^{0}C: (**a**,**b**) deep cryogenic treatment- homogenous formation of cementite within microstructure; (**c**,**d**) shallow cryogenic treatment- inhomogeneous areas of cementite within the microstructure and coarsened precipitated carbides on the boundaries on the grains of tempered martensite.

Based on Figure 13, comparing the microstructures of both cryotreatments via scanning electron microscope, in case of shallow cryotreatment, carbides are finer and more homogeneously distributed

 doi:10.20944/preprints202605.1642.v1

inside the grains of tempered martensite (Figure 13b), compared to carbides' distribution inside the grains of tempered martensite after deep cryotreatment (Figure 13a).

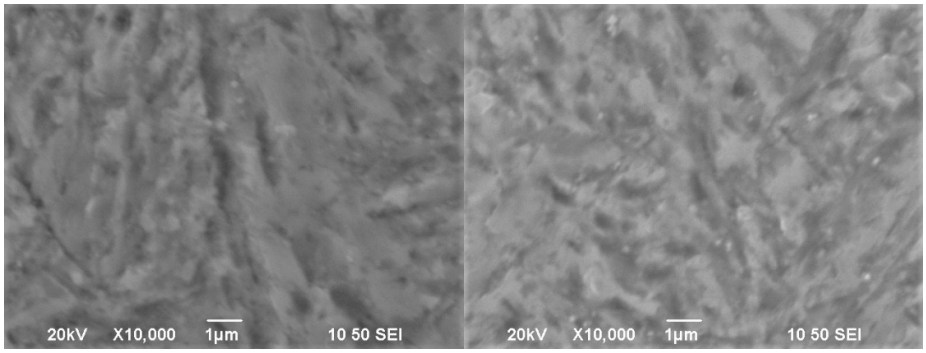

(**a**) (**b**)

Figure 13. Microstructure features after cryotreatment and tempering at 550^{0}C: (**a**) deep cryogenic treatment- finely dispersed sub-micron carbides inside the grains of tempered martensite; (**b**) shallow cryogenic treatment- finer and homogeneously distributed sub-micron carbides inside the grains of tempered martensite.

4. Conclusions

The microstructure of both shallow and deep cryogenically treated-low tempered AISI H13 tool steel is comprised of a matrix of needle-like lath martensite were globular transition and primary carbides are finely dispersed. Retained austenite was also found in the microstructure. Enhanced density of globular carbides is observed to both sub-zero treatments of the specific tool steel grade [70]. It is triggered by different mechanisms· the relatively prolonged holding time of 24h to -196^{0}C in deep cryogenic treatment [20] and the prolonged ramp up time of 30h to -130^{0}C in shallow cryogenic treatment respectively.

Tempering on 500^{0}C (secondary hardening peak) showed that the microstructure of both subzero treatments is comprized of tempered martensite and carbides. The weight percent of retained austenite is less than 5%. In case of deep cryogenic treatment, the carbide precipitation is more pronounced to the grain boundaries of tempered martensite. On the other hand, in case of shallow cryogenic treatment, carbides are homogenically dispersed inside the tempered martensite grains. Evidently, the parameters of the subzero stage through the heat treatment sequence, namely holding time and ramp up rate are critical for the precipitation topology of the secondary carbides which affects the acquired microstructure and its properties [4].

Main features of the microstructure of both cryotreatments of the tool steel grade and after tempering at 525^{0}C are a) formation of cementite within the microstructure and b) carbides precipitation. More specifically, unhomogenous distribution of cementite inside the microstructure is observed in case of shallow cryogenic treated specimen. Through tempering at 525^{0}C, in both subzero treatments, distinct carbides precipitation on both inner and boundary areas of the tempered martensite grains is realized.

In general, cryotreatment and tempering at 550^{0}C, extensive cementite formation is noted as tempered martensite decomposes further provoking microstructural changes and coarsening of carbides are the main features of the acquired microstructure. After shallow cryogenic treatment, there are areas of inhomogenous formation of cementite. In same time, carbides are coarsened on the grain boundaries while they are finer and more distributed inside the grains. The microstructure after deep cryotreatment is more homogenous for both the microstrucure and the dispersion of the carbides respectively.

Different patterns on the evolution of the microstructure after deep and shallow cryogenic treatment is observed. It is evident that prolonged holding time at deep cryogenic temperature leads to a more homogenous microstructure with equaly developed carbide distribution on both inside and the boundaries of the grains in a matrix of tempered martensite. The prolonged ramp up rate

 doi:10.20944/preprints202605.1642.v1

after holding time to shallow cryogenic temperature lead to inhomogenous microstructure having fully developed/coarsened carbides on the grain boundaries while finer, having higher density and finer distribution carbdes inside the grains of tempered martensite.

Thermal hysteresis in case of deep cryogenic treatment and consecutive equilibrium states through warming up in case of shallow cryogenic treatment are the triggering mechanisms of the specific subzero treatments. Based on the evidence, the microstructures acquired are different and will have an impact to the properties of the specific tool steel grade on the macroscopic level.

Author Contributions: Conceptualization, D.G.P.; methodology, D.G.P., A.A. and Di.M.; validation, D.G.P., C.H., Di.M. and D.M.; investigation, D.G.P., A.A. and Di.M.; resources, D.G.P., C.H., Di.M. and D.M.; writing—original draft preparation, D.G.P.; writing—review and editing, D.G.P., Di.M. and D.M.; visualization, D.G.P.; supervision, C.H., Di.M. and D.M. All authors have read and agreed to the published version of the manuscript.

Institutional Review Board Statement: Not applicable.

Informed Consent Statement: Not applicable.

Data Availability Statement: Not applicable.

Acknowledgments: Authors would like to thank Anthi Tsaroucha for the help with the initial preparation of metallographic specimens.

Conflicts of Interest: The authors declare no conflicts of interest.

Abbreviations

The following abbreviations are used in this manuscript:

SCT	Shallow Cryogenic Treatment
DCT	Deep Cryogenic Treatment

References

1. Kalsi, N.S.; Sehgal, R.; Sharma, V.S. Cryogenic Treatment of Tool Materials: A Review. *Mater. Manuf. Process.* **2010**, *25*, 1077–1100, doi:10.1080/10426911003720862.
2. Jawahir, I.S.; Attia, H.; Biermann, D.; Duflou, J.; Klocke, F.; Meyer, D.; Newman, S.T.; Pusavec, F.; Putz, M.; Rech, J.; et al. Cryogenic Manufacturing Processes. *CIRP Ann.* **2016**, *65*, 713–736, doi:10.1016/j.cirp.2016.06.007.
3. Diekman, F. Cold and Cryogenic Treatment of Steel. In *Steel Heat Treating Fundamentals and Processes*; Dossett, J.L., Totten, G.E., Eds.; ASM International, 2013; pp. 382–386 ISBN 978-1-62708-165-8.
4. Villa, M.; Somers, M.A.J. On the Role of Isothermal Martensite Formation during Cryogenic Treatment of Steels: Zur Rolle Der Isothermen Martensitbildung Bei Der Tieftemperaturbehandlung von Stählen. *HTM J. Heat Treat. Mater.* **2020**, *75*, 49–72, doi:10.3139/105.110420.
5. Padmakumar, M.; Dinakaran, D. A Review on Cryogenic Treatment of Tungsten Carbide (WC-Co) Tool Material. *Mater. Manuf. Process.* **2021**, *36*, 637–659, doi:10.1080/10426914.2020.1843668.
6. Moore, K.; Collins, D.N. Cryogenic Treatment of Three Heat-Treated Tool Steels. *Key Eng. Mater.* **1993**, *86–87*, 47–54, doi:10.4028/www.scientific.net/KEM.86-87.47.
7. Collins, D.N. Classic Contributions: Cryogenic Treatment Deep Cryogenic Treatment of Tool Steels: A Review. *Int. Heat Treat. Surf. Eng.* **2008**, *2*, 147–149, doi:10.1179/174951508X446367.
8. Collins, D.N.; Dormer, J. Classic Contributions: Cryogenic Treatment Deep Cryogenic Treatment of a D2 Cold Work Tool Steel. *Int. Heat Treat. Surf. Eng.* **2008**, *2*, 150–154, doi:10.1179/174951508X446376.
9. Yen, P.L.; Kamody, D.J. *Industrial Furnace*. 1997, pp. 40–44.
10. Barron R.F. Cryogenic Treatment of Metals to Improve Wear Resistance. *Cryogenics* **1982**, *22*, 409–413, doi:10.1016/0011-2275(82)90085-6.
11. *Encyclopedia of Iron, Steel, and Their Alloys*; Colás, R., Totten, G.E., Eds.; CRC Press, 2016; ISBN 978-1-4665-1104-0.

 doi:10.20944/preprints202605.1642.v1

12. Jovičević-Klug, P.; Podgornik, B. Review on the Effect of Deep Cryogenic Treatment of Metallic Materials in Automotive Applications. *Metals* **2020**, *10*, 434, doi:10.3390/met10040434.
13. Pellizzari, M.; Molinari, A. Deep Cryogenic Treatment of Cold Work Tool Steel. In Proceedings of the 6th International Tooling Conference; Karlstad University: Karlstad, Sweden, September 10 2002; Vol. 2, pp. 657–669.
14. Taylor, K.A.; Olson, G.B.; Cohen, M.; Sande, J.B.V. Carbide Precipitation during Stage I Tempering of Fe-Ni-C Martensites. *Metall. Trans. A* **1989**, *20*, 2749–2765, doi:10.1007/BF02670168.
15. Zhu, C.; Cerezo, A.; Smith, G.D.W. Carbide Characterization in Low-Temperature Tempered Steels. *Ultramicroscopy* **2009**, *109*, 545–552, doi:10.1016/j.ultramic.2008.12.007.
16. Olson, G.B.; Cohen, M. Interphase-Boundary Dislocations and the Concept of Coherency. *Acta Metall.* **1979**, *27*, 1907–1918, doi:10.1016/0001-6160(79)90081-6.
17. Speich, G.R.; Leslie, W.C. Tempering of Steel. *Metall. Trans.* **1972**, *3*, 1043–1054, doi:10.1007/BF02642436.
18. Ohmori, Y.; Tamura, I. Epsilon Carbide Precipitation during Tempering of Plain Carbon Martensite. *Metall. Trans. A* **1992**, *23*, 2737–2751, doi:10.1007/BF02651753.
19. Gill, S.S.; Singh, J.; Singh, R.; Singh, H. Metallurgical Principles of Cryogenically Treated Tool Steels—a Review on the Current State of Science. *Int. J. Adv. Manuf. Technol.* **2011**, *54*, 59–82, doi:10.1007/s00170-010-2935-5.
20. Collins, D.N.; O'Rourke G The Response of Tool Steels to Deep Cryogenic Treatment Effect of Alloying Elements. In Proceedings of the Heat treating : proceedings of the 18th conference; ASM International, 1999; pp. 229–247.
21. Li, H.; Tong, W.; Cui, J.; Zhang, H.; Chen, L.; Zuo, L. The Influence of Deep Cryogenic Treatment on the Properties of High-Vanadium Alloy Steel. *Mater. Sci. Eng. A* **2016**, *662*, 356–362, doi:10.1016/j.msea.2016.03.039.
22. Molinari, A.; Pellizzari, M.; Gialanella, S.; Straffelini, G.; Stiasny, K.H. Effect of Deep Cryogenic Treatment on the Mechanical Properties of Tool Steels. *J. Mater. Process. Technol.* **2001**, *118*, 350–355, doi:10.1016/S0924-0136(01)00973-6.
23. Jurči, P.; Yarasu, V.; Dlouhý, I.; Bartkowska, A. Optimization of Wear-, Fracture- and Corrosion Performance of Vanadis 6 Steel through Cryogenic Treatment and Tempering. *IOP Conf. Ser. Mater. Sci. Eng.* **2023**, *1284*, 012086, doi:10.1088/1757-899X/1284/1/012086.
24. Shinde, T.; Pruncu, C.; Dhokey, N.B.; Parau, A.C.; Vladescu, A. Effect of Deep Cryogenic Treatment on Corrosion Behavior of AISI H13 Die Steel. *Materials* **2021**, *14*, 7863, doi:10.3390/ma14247863.
25. Jovičević-Klug, P.; Kranjec, T.; Jovičević-Klug, M.; Kosec, T.; Podgornik, B. Influence of the Deep Cryogenic Treatment on AISI 52100 and AISI D3 Steel's Corrosion Resistance. *Materials* **2021**, *14*, 6357, doi:10.3390/ma14216357.
26. Jurči, P.; Dlouhý, I. Cryogenic Treatment of Martensitic Steels: Microstructural Fundamentals and Implications for Mechanical Properties and Wear and Corrosion Performance. *Materials* **2024**, *17*, 548, doi:10.3390/ma17030548.
27. Zurecki, Z. Quenching of Steel Revisited; In Proceedings of the Heat Treating: Proceedings of the 23rd Heat Treating Society Conference; ASM International: Pittchburg, Pensylvania, Usa, September 25 2005; pp. 1–9.
28. Kelkar, R.; Nash, P.; Zhu, Y. *Heat Treating Progress*. pp. 57–60.
29. Caldesi, E.; Carlevaris, D.; Dauriz, A.; Lindholm, S.; Ometto, A.; Zampiccoli, M.; Pellizzari, M. *Heat treatment*. 2019,.
30. Linde AG Sub-Zero Treatment of Steels. Technology/Processes/Equipment 2010.
31. Barron R.F. *Boxboard Containers International-Primedia Business Magazines & Media*. December 1980,.
32. Frey R. Cryogenic Treatment Improves Properties of Drills and P/M Parts. *19*.
33. Cryogenic Processing, Tools and Parts 2007.
34. J. Dosset, G.E. Totten *Steel Heat Treating Fundamentals and Processes*; ASM Metals Handbook; ASM International: Metals Park, Ohio; Vol. 4A;
35. Patil, P.I.; Tated, R.G. Comparison of Effects of Cryogenic Treatment on Different Types of Steels: A Review. *IJCA* **2012**.

 doi:10.20944/preprints202605.1642.v1

36. Blaha, J.; Krempaszky, C.; Werner, E.A.; Liebfahrt, W. Carbide Distribution Effects in Cold Work Tool Steels. In Proceedings of the Proceedings of the 6th International Tooling Conference; karlstad University: Sweden, September 10 2002; pp. 289–297.
37. Papageorgiou, D.G.; Karantonis, A.; Pavlatou, E.; Manolakos, D. Subzero Treatment of Hot Work Tool Steels as a Measure against Failure. *Eng. Fail. Anal.* **2025**, *182*, 110046, doi:10.1016/j.engfailanal.2025.110046.
38. Matteo Villa, Marcel A. J. Somers Cryogenic Treatment of Steel: From Concept to Metallurgical Understanding. In Proceedings of the Proceedings of the 24th IFHTSE Congress; Nice, France, 2017.
39. G.A. Roberts, J.P. Gill Some Effects of Sub-Zero Cooling on the Tempering of High Speed Steel. *Iron age* **1944**, *153*.
40. Oppenkowski, A.; Weber, S.; Theisen, W. Evaluation of Factors Influencing Deep Cryogenic Treatment That Affect the Properties of Tool Steels. *J. Mater. Process. Technol.* **2010**, *210*, 1949–1955, doi:10.1016/j.jmatprotec.2010.07.007.
41. Preciado, M.; Pellizzari, M. Influence of Deep Cryogenic Treatment on the Thermal Decomposition of Fe–C Martensite. *J. Mater. Sci.* **2014**, *49*, 8183–8191, doi:10.1007/s10853-014-8527-2.
42. Jovičević-Klug, P.; Jovičević-Klug, M.; Podgornik, B. Effectiveness of Deep Cryogenic Treatment on Carbide Precipitation. *J. Mater. Res. Technol.* **2020**, *9*, 13014–13026, doi:10.1016/j.jmrt.2020.09.063.
43. Yugandhar T.; Krishnan, P.K.; Rao, C.V.B.; Kalidas R. Cryogenic Treatment and Its Effect on Tool Steel.; Karlstad, Sweden, September 10 2002; Vol. 2, pp. 672–683.
44. Uddeholms AB Uddeholm Sleipner- Technical Data.
45. Papageorgiou, D.; Tsaroucha, A.; Mouzakis, Dion; Manolakos, D. Microstructure Evaluation of Cryogenically Hardened and Tempered 5%Cr Hot Work Tool Steel. In Proceedings of the 7th International Conference of Engineering Against Failure; IOP Publishing Ltd: Greece, June 21 2023.
46. Papadimitriou, G. *General Metallurgy II-The Alloys (in Greek)*; Publications of National Technical University of Athens, 1993;
47. Haidemenopoulos, G.N. *Physical Metallurgy: Principles and Design*; 1st ed.; Taylor & Francis Group: Milton, 2018; ISBN 978-1-138-62768-0.
48. Pérez, M.; Belzunce, F.J. The Effect of Deep Cryogenic Treatments on the Mechanical Properties of an AISI H13 Steel. *Mater. Sci. Eng. A* **2015**, *624*, 32–40, doi:10.1016/j.msea.2014.11.051.
49. Li, S.; Guo, H.; Li, J.; Li, Z.; Li, J. Carbides Precipitation and Kinetics of H13 Steel Subjected to Deep Cryogenic Treatment. *Mater. Sci. Technol.* **2022**, *38*, 1376–1389, doi:10.1080/02670836.2022.2079862.
50. Gecu, R. Combined Effects of Cryogenic Treatment and Tempering on Microstructural and Tribological Features of AISI H13 Steel. *Mater. Chem. Phys.* **2022**, *292*, 126802, doi:10.1016/j.matchemphys.2022.126802.
51. Ning, A.; Liu, Y.; Gao, R.; Yue, S.; Wang, M.; Guo, H. Effect of Austenitizing Condition on Mechanical Properties, Microstructure and Precipitation Behavior of AISI H13 Steel. *J. Iron Steel Res. Int.* **2024**, *31*, 143–156, doi:10.1007/s42243-022-00837-w.
52. Wang, H.; Li, J.; Shi, C.-B.; Li, J.; He, B. Evolution of Carbides in H13 Steel in Heat Treatment Process. *Mater. Trans.* **2017**, *58*, 152–156, doi:10.2320/matertrans.M2016268.
53. Mesquita, R.A.; Kubin, M.; Schneider, R. *Tool Steels: Properties and Performance*; Materials science and engineering; CRC Press, Taylor & Francis Group: Boca Raton London New York, 2017; ISBN 978-1-4398-8171-2.
54. Gavriljuk, V.G.; Sirosh, V.A.; Petrov, Yu.N.; Tyshchenko, A.I.; Theisen, W.; Kortmann, A. Carbide Precipitation During Tempering of a Tool Steel Subjected to Deep Cryogenic Treatment. *Metall. Mater. Trans. A* **2014**, *45*, 2453–2465, doi:10.1007/s11661-014-2202-8.
55. Bhawar, V.; Khot, S.; Kattire, P.; Mehta, M.; Singh, R. Influence of Deep Cryogenic Treatment (DCT) on Thermo Mechanical Performance of AISI H13 Tool Steel. *J. Mater. Sci. Chem. Eng.* **2017**, *05*, 91–101, doi:10.4236/msce.2017.51013.
56. Katoch, S.; Sehgal, R.; Singh, V. Evolution of Mechanical Properties and Microstructure of Differently Cryogenically Treated Hot Die Steel AISI–H13. *Int. J. Mater. Res.* **2017**, *108*, 173–184, doi:10.3139/146.111467.
57. Katoch, S.; Sehgal, R.; Singh, V. Effect of Cryogenic Treatment on Hardness, Microstructure and Wear Behavior of Hot Die Steel Grade AISI-H13. In *Proceedings of International Conference on Advances in Tribology*

 doi:10.20944/preprints202605.1642.v1

and Engineering Systems; Patel, H.C., Deheri, G., Patel, H.S., Mehta, S.M., Eds.; Lecture Notes in Mechanical Engineering; Springer India: New Delhi, 2014; pp. 159–166 ISBN 978-81-322-1655-1.

58. Shinde, T. Influence of Carbide Particle Size on the Wear Performance of Cryogenically Treated H13 Die Steel. *Surf. Eng.* **2021**, *37*, 1206–1214, doi:10.1080/02670844.2019.1701858.
59. Uddeholms AB Uddeholm Orvar 2 Microdized- Technical Data 2021.
60. *Heat Treater's Guide: Practices and Procedures for Irons and Steels*; Chandler, H., Ed.; 2. ed.; ASM International: Metals Park, Ohio, 1995; ISBN 978-0-87170-520-4.
61. E04 Committee ASTM International. *Test Method for Microindentation Hardness of Materials*; DOI: 10.1520/E0384-22.
62. E04 Committee ASTM International. *Guide for Preparation of Metallographic Specimens*; DOI: 10.1520/E0003-01.
63. Kitahara, H.; Ueji, R.; Tsuji, N.; Minamino, Y. Crystallographic Features of Lath Martensite in Low-Carbon Steel. *Acta Mater.* **2006**, *54*, 1279–1288, doi:10.1016/j.actamat.2005.11.001.
64. Tóth, L. Reduction of Retained Austenite in Tool Steels. *Műszaki Tudományos Közlemények* **2022**, *16*, 52–57, doi:10.33894/mtk-2022.16.10.
65. Zare, A.; Hosseini, S.R. Influence of Soaking Time in Deep Cryogenic Treatment on the Microstructure and Mechanical Properties of Low-Alloy Medium-Carbon HY-TUF Steel. *Int. J. Miner. Metall. Mater.* **2016**, *23*, 658–666, doi:10.1007/s12613-016-1278-0.
66. Shinde, T. Influence of Carbide Particle Size on the Wear Performance of Cryogenically Treated H13 Die Steel. *Surf. Eng.* **2021**, *37*, 1206–1214, doi:10.1080/02670844.2019.1701858.
67. Jovičević-Klug, P.; Tóth, L.; Podgornik, B. Comparison of K340 Steel Microstructure and Mechanical Properties Using Shallow and Deep Cryogenic Treatment. *Coatings* **2022**, *12*, 1296, doi:10.3390/coatings12091296.
68. Speich, G.R.; Taylor, K.A. Tempering of Ferrous Martensites. In *Martensite*; ASM International: Materials Park, Ohio, 1992; pp. 243–275 ISBN 0-87170-434-X.
69. Lyman, T.; Boyer, H.; Carnes, W.; Unterwelser, P. *Atlas of Microstructures of Industrial Alloys*; 8th ed.; Americal Society for Metals: Metals Park, Ohio, 1972; Vol. 7; ISBN 978-0-7837-1865-1.
70. Jurči, P.; Ptačinová, J.; Sahul, M.; Dománková, M.; Dlouhy, I. Metallurgical Principles of Microstructure Formation in Sub-Zero Treated Cold-Work Tool Steels – a Review. *Matér. Tech.* **2018**, *106*, 104, doi:10.1051/mattech/2018022.